Supplementary Information

Double Layer Mesoscopic Electron Contact for Efficient Perovskite Solar Cells

Rohit D. Chavan,[a] Pankaj Yadav,[b] Mohammad Mahdi Tavakoli,[c,d] Daniel Prochowicz,[e] Ajaysing Nimbalkar,[a] Sangram P. Bhoite,[a] Popatrao N. Bhosale[f] and Chang Kook Hong[a,*]

[a] *Polymer Energy Materials Laboratory, School of Applied Chemical Engineering, Chonnam National University, Gwangju 500-757, South Korea.*

[b] *Department of Solar Energy, School of Technology, Pandit Deendayal Petroleum University, Gandhinagar-382 007, Gujarat, India.*

[c] *Department of Electrical Engineering and Computer Science, Massachusetts Institute of Technology, Cambridge, MA 02139, USA*

[d] *Department of Materials Science and Engineering, Sharif University of Technology, 14588 Tehran, Iran*

[e] *Institute of Physical Chemistry, Polish Academy of Sciences, Kasprzaka 44/52, 01-224 Warsaw, Poland*

[f] *Materials Research Laboratory, Department of Chemistry, Shivaji University, Kolhapur, India.*

***Corresponding author**

Email: hongck@chonnam.ac.kr (Prof. Chang Kook Hong)

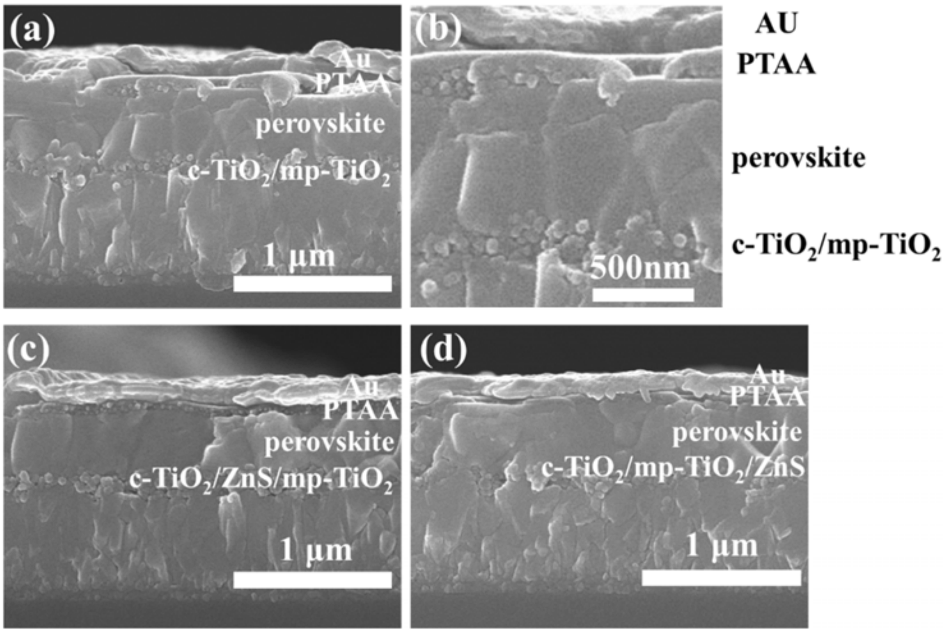

Fig. S1 Cross section SEM images of (a) c-TiO_2/mp-TiO_2, (b) zoom c-TiO_2/mp-TiO_2, (c) c-TiO_2/ZnS and (d) mp-TiO_2/ZnS based PSCs.

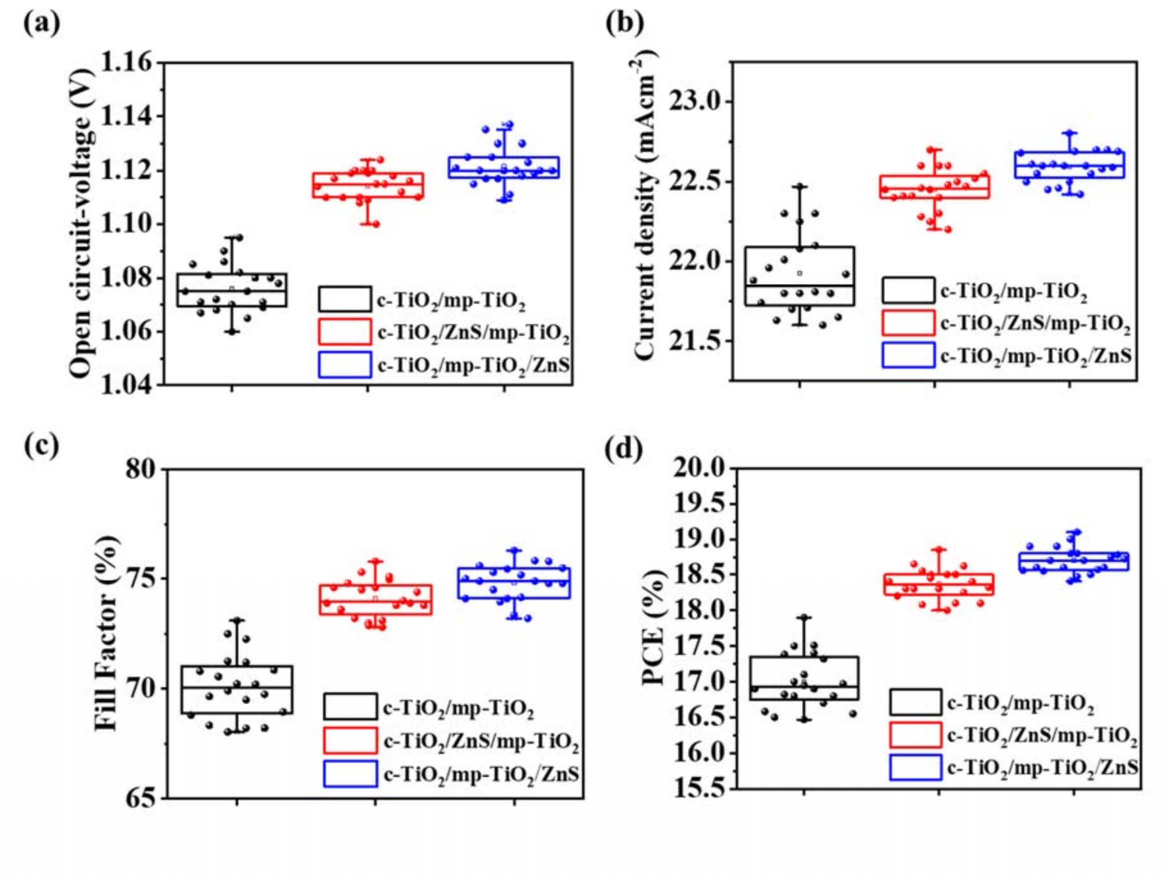

Fig. S2 Statistic histograms of PCE, J_{sc}, V_{oc} and FF from the collected 20 devices extracted from J-V curves of $c\text{-}TiO_2/mp\text{-}TiO_2$, $c\text{-}TiO_2/ZnS/mp\text{-}TiO_2$ and $c\text{-}TiO_2/ZnS/mp\text{-}TiO_2$ based PSCs.

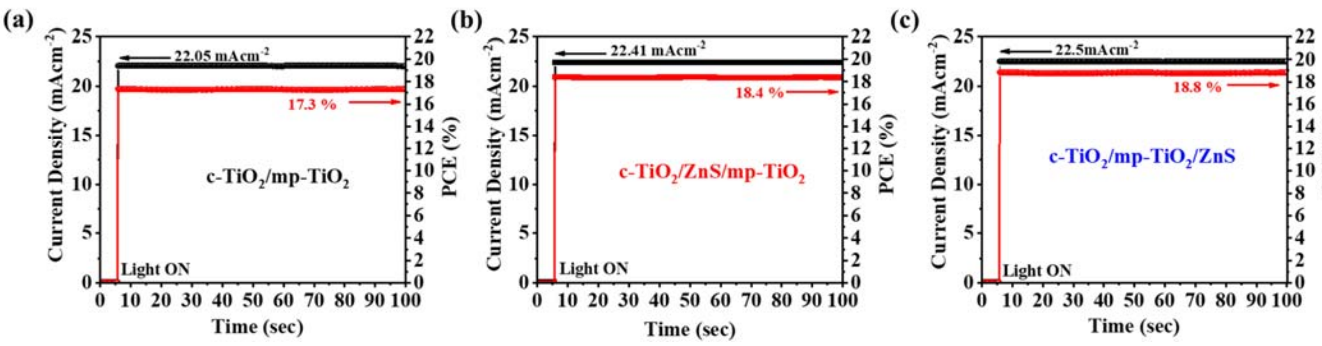

Fig. S3 Steady-state PCE and photocurrent stabilities for (a) $c\text{-}TiO_2/mp\text{-}TiO_2$, (b) $c\text{-}TiO_2/ZnS/mp\text{-}TiO_2$ and (c) $c\text{-}TiO_2/mp\text{-}TiO_2/$ ZnS based devices.

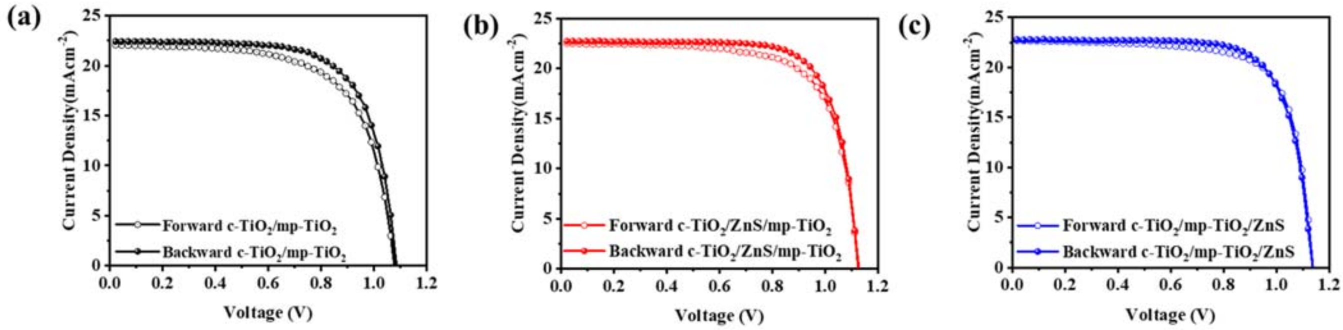

Fig. S4 J-V curves of champion device under both forward and backward scan directions (a) c-TiO_2/mp-TiO_2, (b) c-TiO_2/ZnS/mp-TiO_2 and (c) mp-TiO_2/ZnS based devices.

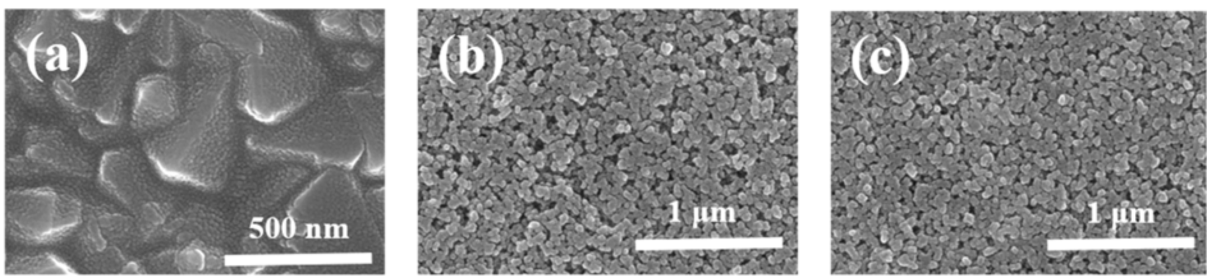

Fig. S5 Top view SEM images of bare (a) FTO/c-TiO_2/ZnS, (b) FTO/c-TiO_2/mp-TiO_2 and (c) FTO/c-TiO_2/mp-TiO_2/ZnS layers.

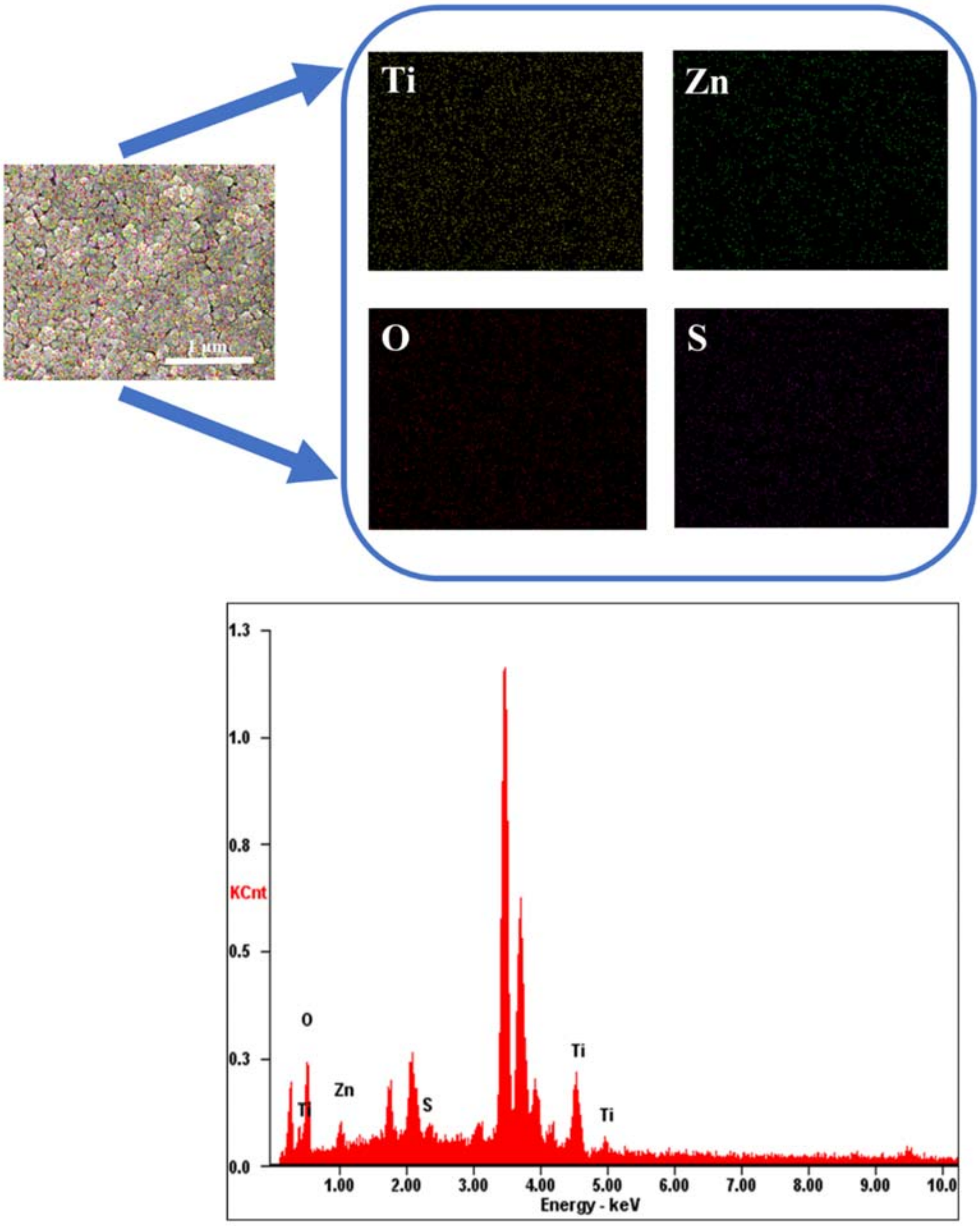

Fig. S6 Energy dispersive X-ray spectroscopy (EDS) elemental mapping and spectrum of Ti, O, Zn and S in FTO/c-TiO_2/mp-TiO_2/ZnS films. The scale bar is 1 μm (mapping images are artificially colored for better observation).

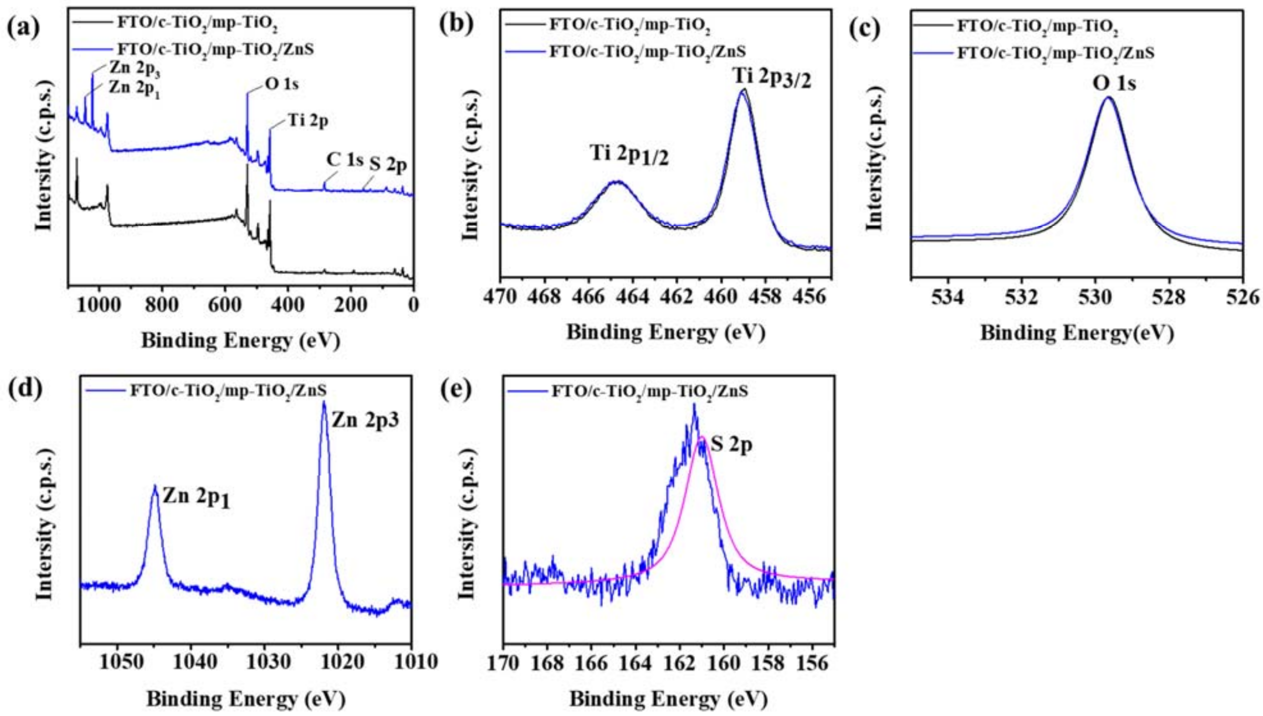

Fig. S7 XPS spectra of (a) FTO/c-TiO_2/mp-TiO_2 and FTO/c-TiO_2/mp-TiO_2/ZnS films. (b) Ti 2p core level spectra of c-TiO_2/mp-TiO_2 and c-TiO_2/mp-TiO_2/ZnS films. (c) O 1s core level spectra of c-TiO_2/mp-TiO_2 and c-TiO_2/mp-TiO_2/ZnS films. (d) Zn 2p core level spectra of c-TiO_2/mp-TiO_2/ZnS film. (e) S 2p core level spectra of c-TiO_2/mp-TiO_2/ZnS film.

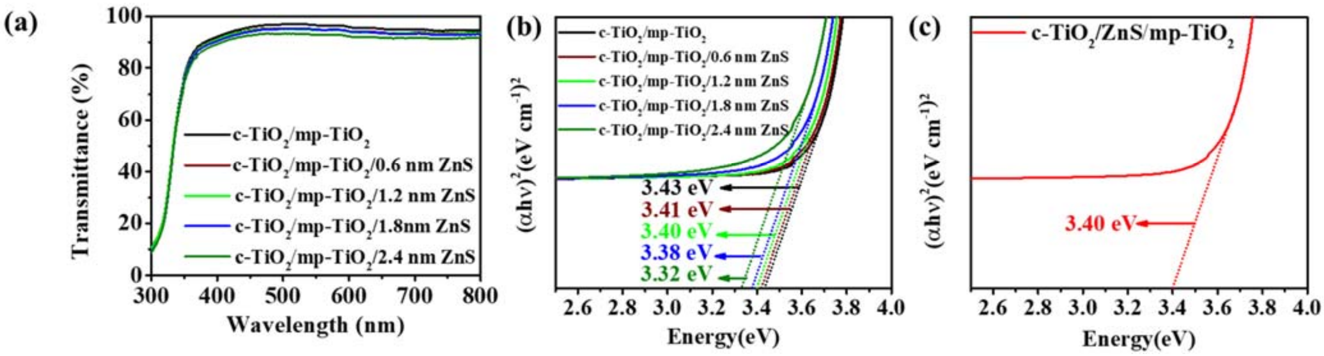

Fig. S8 (a) Transmission spectra of FTO/c-TiO_2/mp-TiO_2 and different ALD cycles of FTO/c-TiO_2/mp-TiO_2/ZnS ETLs films. (b) Tauc plot of $(\alpha h\nu)^2$ vs photon energy of c-TiO_2/mp-TiO_2 and different ALD cycles of c-TiO_2/mp-TiO_2/ZnS ETLs films. (c) Tauc plot of $(\alpha h\nu)^2$ vs photon energy of c-TiO_2/ZnS.

Table S1. Photovoltaic properties of the champion PSCs based on c-TiO_2/mp-TiO_2, c-TiO_2/ZnS/mp-TiO_2 and c-TiO_2/mp-TiO_2/ZnS under AM 1.5G illumination with different ALD cycles of ZnS buffer layer.

ETLs	V_{OC} (V)	J_{SC} (mAcm^{-2})	FF (%)	PCE (%)
c-TiO_2/mp-TiO_2	1.095	22.48	73.10	17.90
c-TiO_2/0.6 nm ZnS/mp-TiO_2	1.110	22.55	74.84	18.40
c-TiO_2/1.2 nm ZnS/mp-TiO_2	1.115	22.68	75.30	18.63
c-TiO_2/1.8 nm ZnS/mp-TiO_2	**1.124**	**22.76**	**75.80**	**18.85**
c-TiO_2/2.4 nm ZnS/mp-TiO_2	1.100	22.49	72.20	18.12

ETLs	V_{OC} (V)	J_{SC} (mAcm^{-2})	FF (%)	PCE (%)
c-TiO_2/mp-TiO_2/0.6 nm ZnS	1.115	22.60	74.90	18.53
c-TiO_2/mp-TiO_2/1.2 nm ZnS	1.118	22.72	75.85	18.90
c-TiO_2/mp-TiO_2/1.8 nm ZnS	**1.137**	**22.80**	**76.13**	**19.10**
c-TiO_2/mp-TiO_2/2.4 nm ZnS	1.120	22.50	75.08	18.15

Table S2. Solar cell parameter from J-V curves recorded under forward and backward scan direction for c-TiO_2/mp-TiO_2, c-TiO_2/ZnS and mp-TiO_2/ZnS devices.

ETLs	Scan direction	V_{OC} (V)	J_{SC} ($mAcm^{-2}$)	FF (%)	PCE (%)	PCE_{avg} (%)	HI (%)
c-TiO_2/mp-TiO_2	**Forward**	1.080	22.15	71.05	17.02	17.5	4.9
	Backward	1.095	22.48	73.10	17.90		
c-TiO_2/ZnS	**Forward**	1.119	22.52	74.55	18.48	18.7	1.96
	Backward	1.124	22.76	75.80	18.85		
mp-TiO_2/ZnS	**Forward**	1.130	22.71	75.62	18.82	19.0	1.45
	Backward	1.137	22.80	76.13	19.10		

Table S3. XPS elemental analysis of FTO/c-TiO_2/mp-TiO_2 ETL.

Name	Start BE	Peak BE	End BE	FWHM (eV)	Atomic %
C1s	291.38	284.6	280.78	4.65	11.38
O1s	537.21	529.63	524.65	2.45	58.68
Ti $2p_{3/2}$	460.81	458.45	453.71	2.53	16.82
Ti $2p_{1/2}$	466.78	464.01	460.65	2.9	13.11

Table S4. XPS elemental analysis of FTO/c-TiO_2/mp-TiO_2/ZnS ETL.

Name	Start BE	Peak BE	End BE	FWHM (eV)	Atomic %
C1s	290.86	284.6	280.95	3.1	19.31
O1s	535.54	529.80	525.39	2.41	41.79
Ti $2p_{3/2}$	461.01	459.17	455.4	2.12	12.92
Ti $2p_{1/2}$	467.47	464.47	460.93	2.7	11.56
Zn $2p_{3/2}$	1025.46	1021.84	1016.95	2.38	5.51
Zn $2p_{1/2}$	1049.47	1044.89	1040.86	2.49	5.44
S $2p_{1/2}$	165.06	161.06	157.5	3.27	3.47

Table S5. Fitted results of TRPL curve of the perovskite film and perovskite film on c-TiO_2/mp-TiO_2; c-TiO_2/ZnS/mp-TiO_2 and c-TiO_2/mp-TiO_2/ZnS layers.

ETL	A_1	A_2	τ_1 (ns)	τ_2 (ns)	<τ> (ns)
glass/perovskite	0.83	0.17	7.1	46.5	29.4
glass/c-TiO_2/mp-TiO_2/perovskite	0.61	0.39	2.36	22.36	19.53
glass/c-TiO_2/ZnS/mp-TiO_2/perovskite	0.65	0.35	4.67	22.84	17.75
glass/c-TiO_2/mp-TiO_2/ZnS/perovskite	0.76	0.24	2.41	11.1	7.6

The observed TRPL decay profile data was fitted to a biexponential function of the form in equation (1).

$$I(t) = I_0 + A_1 \exp\left(-\frac{t-t_0}{\tau_1}\right) + A_2 \exp\left(-\frac{t-t_0}{\tau_2}\right) \qquad \ldots. (1)$$

where τ_1 and τ_2 are first and second order decay times and A_1 and A_2 are respective weight factors of each decay area. The average recombination life time is calculated as $<\tau_{avg}>$ for the respective sample with the help of lifetime values and weight fraction amplitude values (%) using the following equation (2).[1,2]

$$< \tau_{avg} > = \sum_n \frac{\sum A_n \tau_n^2}{\sum_m A_m \tau_m^2} \qquad \ldots. (2)$$

Table S6. Energy level detailed calculated parameters from UPS measurements for c-TiO_2/mp-TiO_2 and c-TiO_2/mp-TiO_2/ZnS ETLs.

ETL	E_{cutoff} (ev)	E_{onset} (ev)	VBM (ev)	CBM (ev)	Eg (ev)
c-TiO_2/mp-TiO_2	17.55	3.77	-7.44	-4.01	3.43
c-TiO_2/mp-TiO_2/ZnS	17.49	3.42	-7.15	-3.77	3.38
perovskite*	-	-	-5.65	-3.92	1.6
PTAA*	-	-	-5.1	-1.8	-

* as per standard reference

The Fermi level, VBM and CBM was calculated from the following equation

$$h\nu - \phi = \mathrm{EFermi} - \mathrm{Ecutoff} \quad \ldots. (1)$$

$$\mathrm{VBM} = h\nu + (\mathrm{EFermi} - \mathrm{Ecutoff}) \quad \ldots. (2)$$

$$\mathrm{CBM} = \mathrm{VBM} + \mathrm{Eg} \quad \ldots. (3)$$

Where hν is the energy of the HeI emission line (21.22 eV) and ϕ is the work function of the sample, more detailed for calculations of VBM and CBM can be found Elsevier.[3,4]

REFERENCES

1 S. D. Stranks, G. E. Eperon, G. Grancini, C. Menelaou, M. J. P. Alcocer, T. Leijtens, L. M. Herz, A. Petrozza and H. J. Snaith, *Science*, 2013, **342**, 341–344.

2 J. You, Z. Hong, Y. (Michael) Yang, Q. Chen, M. Cai, T. Song, C. Chen, S. Lu, Y. Liu, H. Zhou and Y. Yang, *ACS Nano*, 2014, **8**, 1674–1680.

3 J. Liu, C. Gao, L. Luo, Q. Ye, X. He, L. Ouyang, X. Guo, D. Zhuang, C. Liao, J. Mei and W. Lau, *J. Mater. Chem. A*, 2015, **3**, 11750–11755.

4 X. Gao, Q. Ge, D. Xue, J. Ding, J. Ma, Y. Chen, B. Zhang, Y. Feng, L. Wan and J. Hu, *Nanoscale*, 2016, **8**, 16881–16885.